

University of Groningen

Predicting future left anterior descending artery events from non-culprit lesions

Kuku, Kayode O.; Garcia-Garcia, Hector M.; Doros, Gheorghe; Mintz, Gary S.; Ali, Ziad A.; Skinner, William H.; Artis, Andre K.; Ten Cate, Tim; Powers, Eric; Wong, Shing Chiu

Published in:

European Heart Journal - Cardiovascular Imaging

DOI:

[10.1093/ehjci/jeab160](https://doi.org/10.1093/ehjci/jeab160)

IMPORTANT NOTE: You are advised to consult the publisher's version (publisher's PDF) if you wish to cite from it. Please check the document version below.

Document Version

Publisher's PDF, also known as Version of record

Publication date:
2022

[Link to publication in University of Groningen/UMCG research database](#)

Citation for published version (APA):

Kuku, K. O., Garcia-Garcia, H. M., Doros, G., Mintz, G. S., Ali, Z. A., Skinner, W. H., Artis, A. K., Ten Cate, T., Powers, E., Wong, S. C., Wykrzykowska, J., Dube, S., Kazziha, S., van der Ent, M., Shah, P., Sum, S., Torguson, R., Di Mario, C., & Waksman, R. (2022). Predicting future left anterior descending artery events from non-culprit lesions: insights from the Lipid-Rich Plaque study. *European Heart Journal - Cardiovascular Imaging*, 23(10), 1365-1372. <https://doi.org/10.1093/ehjci/jeab160>

Copyright

Other than for strictly personal use, it is not permitted to download or to forward/distribute the text or part of it without the consent of the author(s) and/or copyright holder(s), unless the work is under an open content license (like Creative Commons).

The publication may also be distributed here under the terms of Article 25fa of the Dutch Copyright Act, indicated by the "Taverne" license. More information can be found on the University of Groningen website: <https://www.rug.nl/library/open-access/self-archiving-pure/taverne-amendment>.

Take-down policy

If you believe that this document breaches copyright please contact us providing details, and we will remove access to the work immediately and investigate your claim.

Downloaded from the University of Groningen/UMCG research database (Pure): <http://www.rug.nl/research/portal>. For technical reasons the number of authors shown on this cover page is limited to 10 maximum.

Predicting future left anterior descending artery events from non-culprit lesions: insights from the Lipid-Rich Plaque study

Kayode O. Kuku^{1†}, Hector M. Garcia-Garcia  ^{1*†}, Gheorghe Doros¹, Gary S. Mintz¹, Ziad A. Ali², William H. Skinner³, Andre K. Artis⁴, Tim ten Cate⁵, Eric Powers⁶, Shing-Chiu Wong⁷, Joanna Wykrzykowska^{8,9}, Sandeep Dube¹⁰, Samer Kazziha¹¹, Martin van der Ent¹², Priti Shah¹³, Stephen Sum¹³, Rebecca Torguson¹⁴, Carlo Di Mario¹⁵, and Ron Waksman¹; on behalf of the LRP Investigators

¹Section of Interventional Cardiology, Department of Cardiology, MedStar Washington Hospital Center, 110 Irving St NW, Suite 4B1, Washington, DC 20010, USA; ²DeMatteis Cardiovascular Institute, Department of Cardiology, St. Francis Hospital & Heart Center, 100 Port Washington Blvd, Roslyn, NY 11576, USA; ³Department of Cardiology, Baptist Health Lexington, 1740 Nicholasville Road, Lexington, KY 40503, USA; ⁴Department of Cardiology, Methodist Hospitals, 5800 Broadway, Merrillville, IN 46410, USA;

⁵Department of Cardiology, Radboud University Medical Centre, Geert Goopteplein Zuid 10, 6525 GA Nijmegen, Netherlands; ⁶Department of Cardiology, MUSCH Health, West Ashley Medical Pavilion, 2060 Sam Rittenberg Blvd., Charleston, SC 29407, USA; ⁷Department of Cardiology, New York-Presbyterian/Weill Cornell Medical Center, 20 E. 70th St., Starr Pavilion, 4th Floor, New York, NY 10021, USA; ⁸Department of Cardiology, Academic Medical Center, Meibergdreef 9, 1105 AZ Amsterdam, Netherlands;

⁹Department of Cardiology, University of Groningen, University Medical Center Groningen, Hanzeplein 1, 9713 GZ Groningen, Netherlands; ¹⁰Department of Cardiology, Community Heart and Vascular Care, 8075 N. Shadeland Ave., Suite 200, Indianapolis, IN 46250, USA; ¹¹Department of Cardiology, Henry Ford Macomb Hospital, 15855 19 Mile Rd, Clinton Twp, MI 48038, USA; ¹²Department of Cardiology, Maaststad Ziekenhuis, Maastweg 21, 3079 DZ Rotterdam, Netherlands; ¹³Department of Clinical Research and Regulatory, Infraredx, Inc., 28 Crosby Dr., Bedford, MA 01730, USA; ¹⁴Department of Medicine, The Zena and Michael A. Wiener Cardiovascular Institute, Icahn School of Medicine at Mount Sinai, 1 Gustave L. Levy Pl, New York, NY 10029, USA; and ¹⁵Structural Interventional Cardiology, Department of Clinical and Experimental Medicine, Careggi University Hospital, Largo Giovanni Alessandro Brambilla, 3, 50134 Firenze FI, Italy

Received 5 May 2021; editorial decision 29 July 2021; accepted 30 July 2021; online publish-ahead-of-print 19 August 2021

Aims

The left anterior descending (LAD) artery is the most frequently affected site by coronary artery disease. The prospective Lipid Rich Plaque (LRP) study, which enrolled patients undergoing imaging of non-culprits followed over 2 years, reported the successful identification of coronary segments at risk of future events based on near-infrared spectroscopy-intravascular ultrasound (NIRS-IVUS) lipid signals. We aimed to characterize the plaque events involving the LAD vs. non-LAD segments.

Methods and results

LRP enrolled 1563 patients from 2014 to 2016. All adjudicated plaque events defined by the composite of cardiac death, cardiac arrest, non-fatal myocardial infarction, acute coronary syndrome, revascularization by coronary bypass or percutaneous coronary intervention, and rehospitalization for angina with >20% stenosis progression and reported as non-culprit lesion-related major adverse cardiac events (NC-MACE) were classified by NIRS-IVUS maxLCBI_{4 mm} (maximum 4-mm Lipid Core Burden Index) ≤ 400 or > 400 and association with high-risk-plaque characteristics, plaque burden $\geq 70\%$, and minimum lumen area (MLA) $\leq 4 \text{ mm}^2$. Fifty-seven events were recorded with more lipid-rich plaques in the LAD vs. left circumflex and right coronary artery; 12.5% vs. 10.4% vs. 11.3%, $P = 0.097$. Unequivocally, a maxLCBI_{4 mm} > 400 in the LAD was more predictive of NC-MACE [hazard ratio (HR) 4.32, 95% confidence interval (CI) (1.93–9.69); $P = 0.0004$] vs. [HR 2.56, 95% CI (1.06–6.17); $P = 0.0354$] in non-LAD segments. MLA $\leq 4 \text{ mm}^2$ within the maxLCBI_{4 mm} was significantly higher in the LAD (34.1% vs. 25.9% vs. 13.7%, $P < 0.001$).

Conclusion

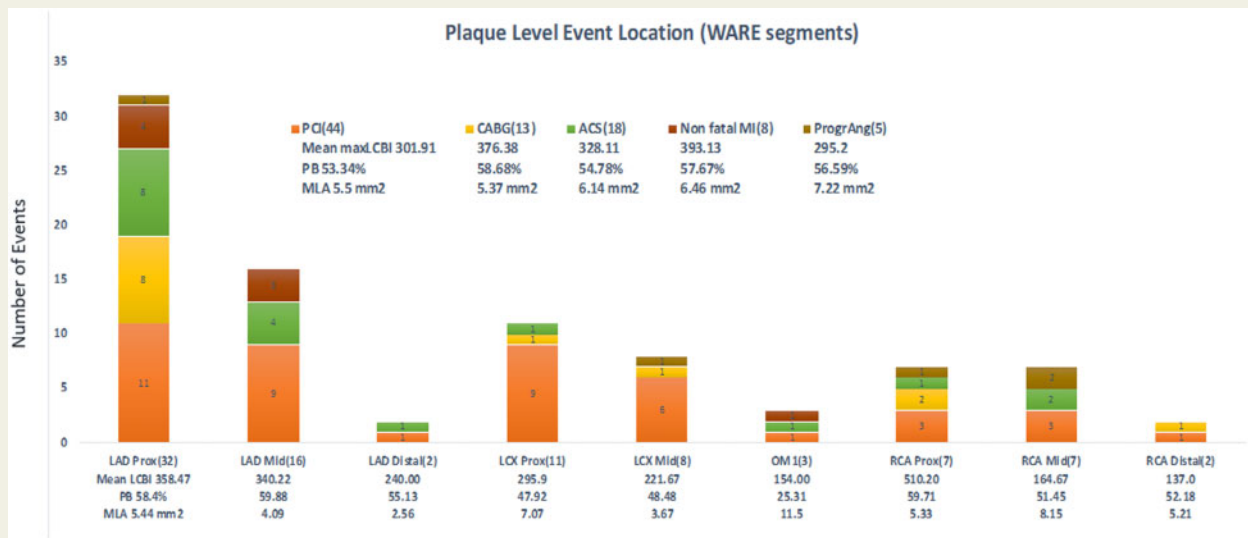
Non-culprit lipid-rich segments in the LAD were more frequently associated with plaque-level events. LAD NIRS-IVUS screening may help identify patients requiring intensive surveillance and medical treatment.

* Corresponding author. Tel: +1 202 877 7754. E-mail: hector.m.garciagarcia@medstar.net; hect2701@gmail.com

† These authors contributed equally to this work.

Published on behalf of the European Society of Cardiology. All rights reserved. © The Author(s) 2021. For permissions, please email: journals.permissions@oup.com.

Graphical Abstract



Keywords

lipid-rich plaque • coronary artery disease • left anterior descending artery • plaque events near-infrared spectroscopy • intravascular ultrasound

Introduction

Coronary artery disease (CAD) plaques are more frequently seen in the left anterior descending (LAD) artery and have a predilection for the proximal segments.^{1–3} A ruptured plaque in the LAD resulting in an acute anterior wall myocardial infarction (MI) is associated with low left ventricular ejection fraction and a worse prognosis.^{4,5} The Lipid Rich Plaque (LRP) study⁶ showed an association between high-risk plaque characteristics detected by intracoronary near-infrared spectroscopy (NIRS)-intravascular ultrasound (IVUS)—including a NIRS-derived $\text{maxLCBI}_{4\text{ mm}} > 400$ and an IVUS plaque burden (PB) $\geq 70\%$ or minimum lumen area (MLA) $\leq 4\text{ mm}^2$ —and subsequent coronary events. However, there has been no natural history study exploring the hypothesis of whether lipid-rich plaques, as assessed by NIRS-IVUS, located in the LAD are associated with more future events as compared to other vessels, which is the objective of the current analysis from the LRP study.

Methods

The design of the LRP study has been reported elsewhere.⁷ Briefly, the LRP study was an international, multicentre, prospective cohort study conducted in patients with suspected CAD who underwent cardiac catheterization with possible *ad hoc* percutaneous coronary intervention (PCI) for an index event. Following successful PCI, additional NIRS-IVUS imaging data were obtained in at least 50 mm of the non-stented segment from two or more major coronary arteries. Plaque-level events were collected in the subsequent 2 years. Ethics committees at the enrolling centres approved the study protocol, and all participants provided written informed consent.

Coronary angiography analysis and NIRS-IVUS imaging protocol and analysis

All quantitative coronary angiographic analysis was done via offline software, CAAS Workstation 7.3 (Pie Medical Imaging BV, Maastricht, The Netherlands) by an independent core laboratory [Angiographic and Invasive Imaging Core Lab, MedStar Cardiovascular Research Network (MCRN), Washington, DC, USA].

NIRS-IVUS was performed using a 3.2-Fr imaging probe with a 40-MHz ultrasound transducer, rotated at 960 rpm (16 fps) to acquire 160 NIRS spectra per second with a pullback speed of 0.5 mm/s (Infraredx, a Nipro Company, Bedford, MA, USA). All the site-blinded non-culprit scans were un-blinded by the core lab and assessed using validated NIRS-IVUS offline analysis software—QIVUS (version 3.0.16.0, Medis Medical Imaging Systems, The Netherlands). All NIRS information was displayed on an automatically generated signal map known as the ‘chemogram’, which indicated the location of lipid-rich plaque within the vessel wall. A quantitative image metric is automatically reported as a numerical Lipid Core Burden Index (LCBI), which represents the fraction of the chemogram yellow pixels that are yellow times 1000.

Each coronary artery with available NIRS-IVUS imaging was divided into 30-mm segments (also referred to as ‘Ware’ segments) beginning from the ostium of the vessel. The proximal segment was defined by the first 30 mm of the NIRS chemogram obtained in the vessel, the mid-segment as the next 30 mm, and the distal segment as the remaining chemogram ≤ 30 mm in length. If the total length of the imaged vessel exceeded 90 mm, the segment beyond 90 mm was defined as the ‘far distal’ segment. Additionally, each 30-mm coronary ‘Ware’ segment was further sub-divided into 10-mm subsegments. Once this segmentation was completed, the software automatically computed the maximum 2- and 4-mm LCBI within each ‘Ware’ segment. LCBI is a quantitative summary metric of lipid within a scanned or selected region. The $\text{maxLCBI}_{4\text{ mm}}$ was

defined as the maximum LCBI of the 4-mm region within the greatest lipid burden.

The greyscale IVUS frames corresponding to the $\text{maxLCBI}_{4\text{ mm}}$ segment were analysed. Vessel and lumen areas were drawn at 1-mm intervals. The difference between the vessel and lumen areas was the plaque area, and PB was the ratio of the plaque to the vessel area.

Study endpoints and definitions

An independent Clinical Events Committee at the Cleveland Clinic Coordinating Center for Clinical Research (CSCR, Cleveland, OH, USA) that was blinded to the NIRS-IVUS findings adjudicated the primary outcome events, defined as the composite of non-fatal MI, acute coronary syndrome (ACS), revascularization by coronary artery bypass grafting (CABG) or PCI, and rehospitalization for angina with $>20\%$ stenosis progression. Together these events were reported as non-culprit lesion-related major adverse cardiac events (NC-MACE).

Statistical analysis

Prespecified subgroups of segments were defined according to LAD (vs. non-LAD) with $\text{maxLCBI}_{4\text{ mm}} \leq 400$ vs. >400 . For categorical variables, frequencies and proportions were used to summarize categorical data. For tabular summaries of proportions, the denominator was the number of subjects with non-missing data. χ^2 or Fisher's exact tests and ANOVA F-tests were used to test the equality of baseline plaque characteristics across four groups (LAD with $\text{maxLCBI}_{4\text{ mm}} \leq 400$; LAD with $\text{maxLCBI}_{4\text{ mm}} > 400$; non-LAD with $\text{maxLCBI}_{4\text{ mm}} \leq 400$; non-LAD with $\text{maxLCBI}_{4\text{ mm}} > 400$). NC-MACE rates were depicted using the Kaplan-Meier (KM) method and compared using the likelihood-ratio test, which accounts for the clustering of plaques within patients. For the plaque-level association of NC-MACE with $\text{maxLCBI}_{4\text{ mm}} \leq 400$ vs. >400 in LAD and non-LAD locations, a random-effect Cox regression model, with a random effect for patients, was used, with $\text{maxLCBI}_{4\text{ mm}}$, LAD vessel indicator, and interaction between them while adjusting for PB within $\text{maxLCBI}_{4\text{ mm}}$ ($\geq 70\%$ vs. $<70\%$) and MLA within $\text{maxLCBI}_{4\text{ mm}}$ ($\leq 4\text{ mm}^2$ vs. $>4\text{ mm}^2$). The proportionality of the hazards assumption was tested for each predictor in the model using the Kolmogorov-type Supremum test for proportional hazards assumption. No significant evidence was found that the proportionality assumption does not hold. All analyses were performed using SAS software, version 9.4 (SAS Institute, Cary, NC, USA). The data underlying this article will be shared on reasonable request to the corresponding author.

Results

From February 2014 through March 2016, a total of 1563 patients were enrolled in the main LRP study. After excluding patients without analysable NIRS ($n = 11$), 281 patients with $\text{maxLCBI}_{4\text{ mm}} < 250$ (who per study design were randomly excluded from the follow-up) and evaluable age at the time of catheterization, a total of 1269 patients (and 5749 Ware segments) were followed through 24 months. In the overall population (irrespective of follow-up allocation), lipid-rich plaques ($\text{maxLCBI}_{4\text{ mm}} > 400$) were present in 11.5% of the imaged plaques, of which 1% had a PB $\geq 70\%$ and 27% had an MLA $\leq 4\text{ mm}^2$ (Supplementary data online, Table S1).

As shown in Table 1, mean patient age and the percentage of male participants were similar across all four groups: (i) non-LAD and $\text{maxLCBI}_{4\text{ mm}} > 400$, (ii) LAD and $\text{maxLCBI}_{4\text{ mm}} > 400$, (iii) non-LAD and $\text{maxLCBI}_{4\text{ mm}} \leq 400$, and (iv) LAD and $\text{maxLCBI}_{4\text{ mm}} \leq 400$. Of note, the percentage of patients with diabetes mellitus was higher in

the two groups with $\text{maxLCBI}_{4\text{ mm}} > 400$. Numerically, we observed more lipid-rich plaques in the LAD than in the left circumflex (LCX) and right coronary artery (RCA): 12.5% vs. 10.4% and 11.3%, respectively, $P = 0.097$. The number of plaques with PB $\geq 70\%$ within the $\text{maxLCBI}_{4\text{ mm}}$ in the RCA was 1.6%, followed by the LAD (1.1%) and LCX (0.6%). An MLA $\leq 4\text{ mm}^2$ within the $\text{maxLCBI}_{4\text{ mm}}$ was observed more in the LAD and LCX than in the RCA: 34.1% vs. 25.9% vs. 13.7%, respectively, $P < 0.001$ (Supplementary data online, Table S1).

There were 57 plaque-level events through the 2-year follow-up period. Lipid-rich plaque ($\text{maxLCBI}_{4\text{ mm}} > 400$) was present in 20/57 (35.1%), a large PB ($\geq 70\%$) was present in 6/57 (10.5%), and a small MLA ($\leq 4\text{ mm}^2$) was present in 26/57 (45.6%). Combining these plaque characteristics, 11/57 (19.3%) of the events were in segments with lipid-rich plaques and a small MLA (defined as $<4.0\text{ mm}^2$); 5/57 (8.8%) were in segments with lipid-rich plaques and a large PB ($\geq 70\%$), and 4 (7%) had all three high-risk plaque characteristics.

Figure 1 shows the major events and their locations. There were 44 PCIs and 13 CABGs. The mean $\text{maxLCBI}_{4\text{ mm}}$ of the Ware segments treated with PCI was 301.9 ± 195.6 and with CABG was 376.4 ± 240.4 . The second most common event type was ACS ($n = 18$), which had a mean $\text{maxLCBI}_{4\text{ mm}}$ of 328.1 ± 224.5 . The Ware segments associated with eight non-fatal MI had a $\text{maxLCBI}_{4\text{ mm}}$ of 393.1 ± 264.6 , the largest observed among the plaque events. Patients who underwent CABG events had the largest average PB (58.68%) and smallest average MLA (5.37 mm^2); non-fatal MI, conversely, occurred in those plaques with the largest average LCBI (Figure 1).

More than half of the plaque events occurred in the LAD, followed by the LCX and RCA (Table 2). Revascularizations were the most common plaque events, and nearly half were performed in the LAD. All non-fatal MIs but one were located in the LAD (in the proximal or midsegments) (Figure 1). As shown in Figure 2, in each of the three vessels (LAD, LCX, and RCA), events were more commonly associated with lesions with a $\text{maxLCBI}_{4\text{ mm}} > 400$ or a PB $\geq 70\%$, although the number of events and differences was greater in the LAD than in the LCX or RCA. A $\text{maxLCBI}_{4\text{ mm}} > 400$ was predictive of NC-MACE both for LAD location [hazard ratio (HR) 4.32, 95% confidence interval (CI) (1.93–9.69); $P = 0.0004$] and for non-LAD location [HR 2.56, 95% CI (1.06–6.17); $P = 0.0354$]. In Supplementary data online, Figure S1, the KM curves by vessel location according to the MLA $\leq 4\text{ mm}^2$ are given. Case examples of patients with high-risk plaques are shown in Figures 3 and 4.

Discussion

The main findings of this report are as follows: (i) plaque-level events were commonly found in acknowledged culprit sites such as LAD and proximal locations; the plaque-level events were more frequently observed in untreated lipid-rich plaques. (ii) Revascularizations were the most common plaque events, and nearly half were performed in the LAD. All non-fatal MIs but one were located in the LAD.

In a pooled analysis of 5250 patients, thrombotic lesions, as detected by coronary angiography, were present more frequently in the LAD and RCA in their proximal segments.¹ It has been proposed that the local shear stress conditions favour the accumulation of lipid

Table I Baseline characteristics

Characteristic	Overall (N = 1269)	Non-LAD and maxLCBI _{4 mm} ≤ 400 (N = 380)	Non-LAD and maxLCBI _{4 mm} > 400 (N = 245)	LAD and maxLCBI _{4 mm} ≤ 400 (N = 391)	LAD and maxLCBI _{4 mm} > 400 (N = 253)	P-value
Age (years), mean ± SD	64 ± 10	65 ± 10	64 ± 11	64 ± 10	63 ± 11	0.572
Male, n (%)	882 (69.5)	279 (73.4)	158 (64.5)	273 (69.8)	172 (68)	0.114
Diabetes mellitus, n (%)	464 (36.7)	115 (30.3)	108 (44.3)	133 (34)	108 (43.4)	<0.001
Diabetes requiring insulin, n (%)	162 (13.1)	33 (8.8)	48 (19.9)	43 (11.3)	38 (15.6)	<0.001
History of smoking, n (%)	685 (54.9)	197 (52.4)	118 (49.6)	220 (57.1)	150 (60.5)	0.056
Current smoker, n (%)	282 (22.6)	80 (21.3)	54 (22.7)	84 (21.8)	64 (25.8)	0.579
Hypertension, n (%)	1018 (80.5)	306 (80.7)	199 (81.6)	311 (79.7)	202 (80.2)	0.951
Family history of CAD, n (%)	636 (56.1)	180 (53.7)	125 (58.1)	204 (57.1)	127 (56.2)	0.733
Prior MI, n (%)	294 (23.5)	94 (25.1)	59 (24.6)	85 (21.9)	56 (22.5)	0.705
Prior PCI, n (%)	567 (44.8)	185 (48.7)	114 (47.1)	160 (40.9)	108 (42.9)	0.133
Presentation with ACS, n (%)	214 (16.9)	51 (13.4)	43 (17.6)	66 (16.9)	54 (21.3)	0.075
Chronic renal insufficiency, n (%)	101 (8)	27 (7.1)	27 (11.1)	26 (6.7)	21 (8.3)	0.204
Hyperlipidaemia, n (%)	1011 (80.3)	307 (81.6)	185 (76.4)	314 (80.5)	205 (81.7)	0.389
PCI during index, n (%)	1110 (87.5)	347 (91.6)	210 (85.7)	336 (85.9)	217 (85.8)	0.046
≥50 mm of eligible vessel, n (%)	1135 (89.4)	340 (89.5)	222 (90.6)	335 (85.7)	238 (94.1)	0.008
Imaged vessel length (mm), mean ± SD	97.893 ± 43.379	91.646 ± 40.813	107.192 ± 44.211	88.924 ± 40.565	112.132 ± 45.308	<0.001
MaxLCBI _{4 mm} , mean ± SD	359.638 ± 174.884	254.524 ± 111.531	535.539 ± 103.798	254.606 ± 107.756	509.498 ± 142.746	<0.001
Avg LCBI _{4 mm} , ^a mean ± SD	220.577 ± 135.204	149.365 ± 87.701	327.623 ± 131.745	162.869 ± 89.522	313.059 ± 136.611	<0.001
Ware segment per patient, mean ± SD	4.533 ± 1.735	4.355 ± 1.69	4.914 ± 1.808	4.148 ± 1.639	5.024 ± 1.695	<0.001

ACS, acute coronary syndrome; CAD, coronary artery disease; LAD, left anterior descending; LCBI, lipid core burden index; MI, myocardial infarction; PCI, percutaneous coronary intervention; SD, standard deviation.

^aAverage maxLCBI_{4 mm} across all Ware segments per patient.

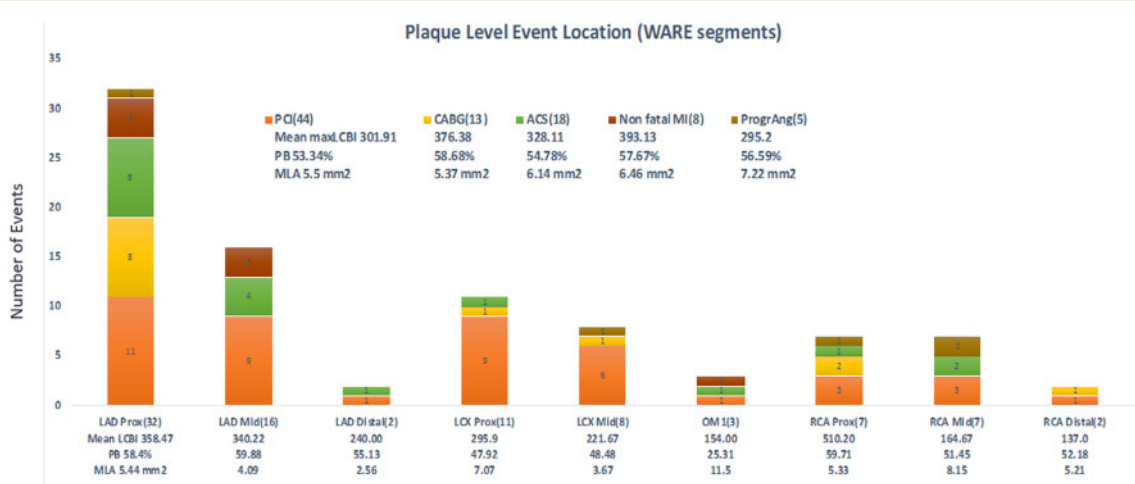


Figure I Number of events in each of the coronary vessel locations. The number in brackets is the number of plaque-level events. ACS, acute coronary syndrome (in green); CABG, coronary artery bypass graft (in yellow); LAD, left anterior descending; LCBI, Lipid Core Burden Index (the number represents the mean of maxLCBI_{4 mm}); LCX, left circumflex; MI, myocardial infarction (in dark red); MLA, minimum lumen area; OM, obtuse marginal; PB, plaque burden; PCI, percutaneous coronary intervention (in orange); ProgrAng, progressive angina (in brown); Prox, proximal; RCA, right coronary artery. *Ware segment may be associated with multiple event types.

Table 2 Distribution of 57 plaque-level events by clinical event type and their angiographic location

Vessel	Any event	PCI ^a	CABG	ACS	Non-fatal MI	Progressive angina
LAD	29/57 (50.9%)	21/43 (48.8%)	8/13 (61.5%)	13/18 (72.2%)	7/8 (87.5%)	1/5 (20%)
LCX	18/57 (31.6%)	15/43 (34.9%)	2/13 (15.4%)	2/18 (11.1%)	1/8 (12.5%)	1/5 (20%)
RCA	10/57 (17.5%)	7/43 (16.3%)	3/13 (23.1%)	3/18 (16.7%)	0/8 (0.0%)	3/5 (60%)

Plaque events may be associated with multiple event types.

ACS, acute coronary syndrome; CABG, coronary artery bypass graft; LAD, left anterior descending; LCX, left circumflex; MI, myocardial infarction; OM, obtuse marginal; PCI, percutaneous coronary intervention; RCA, right coronary artery.

^aSingle OM1 not included in PCI count in comparison with Figure 1.

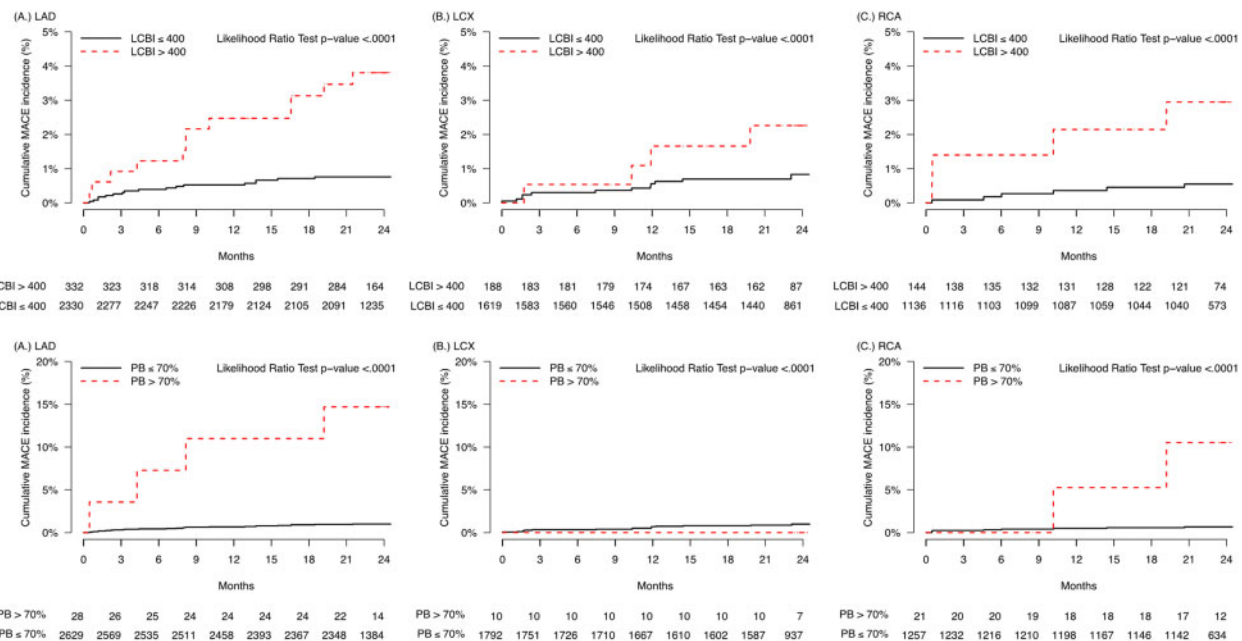


Figure 2 (Top row, A-C) Kaplan-Meier curves for patients with $\text{maxLCBI}_{4\text{ mm}} > 400$ or not in the (A) LAD, (B) LCX, and (C) RCA; (Bottom row, A-C) Kaplan-Meier curves for patients with plaque burden $\geq 70\%$ or not in the (A) LAD, (B) LCX, and (C) RCA. LAD, left anterior descending; LCBI, Lipid Core Burden Index; LCX, left circumflex; MACE, major adverse cardiac events; PB, plaque burden; RCA, right coronary artery.

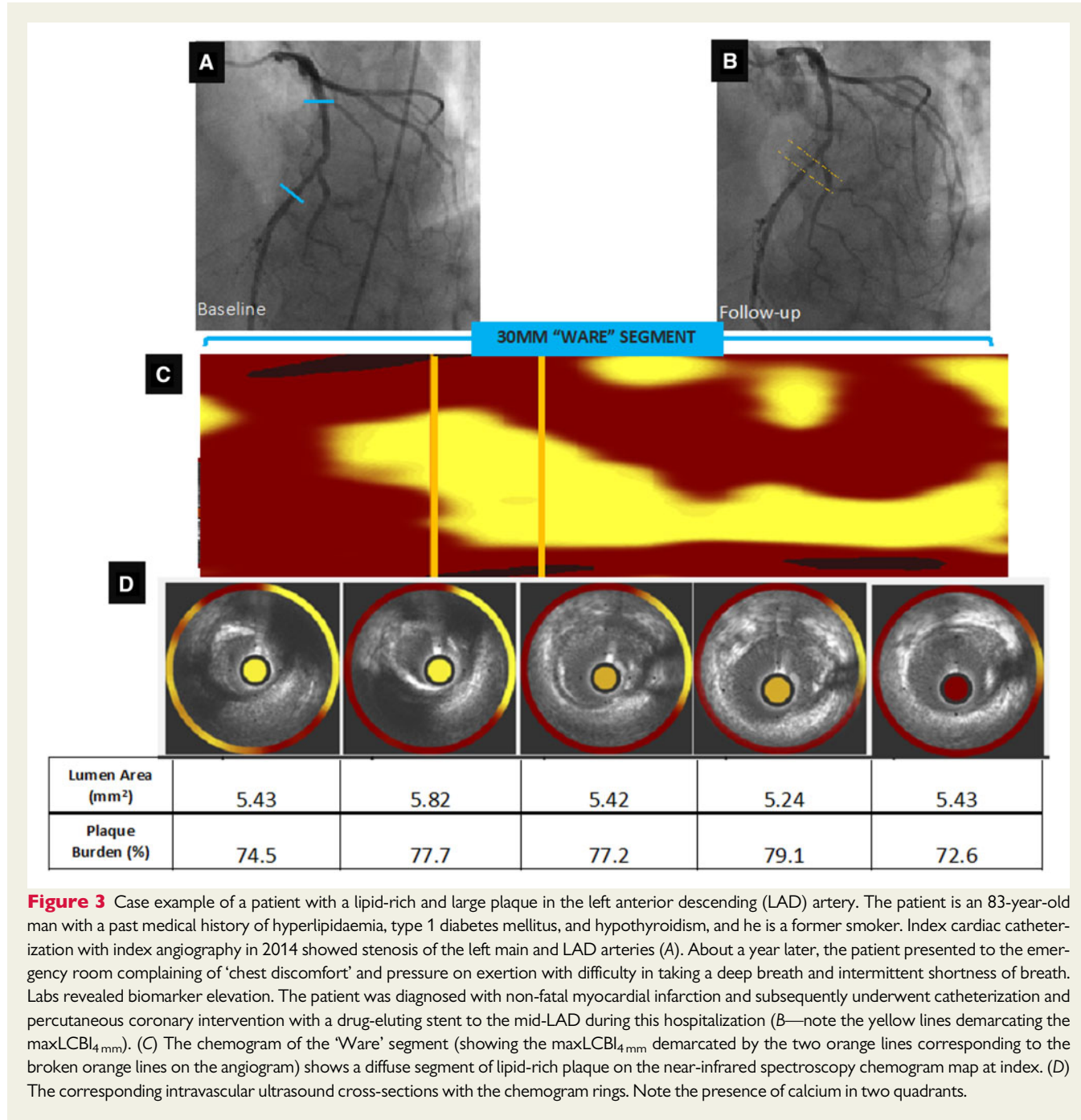
within the vessel wall in these areas.⁸ Particularly in the proximal segment of the LAD, the plaque is mostly located opposite to the takeoff of the LCX, sparing the carina, which makes them eccentric plaques in this location. IVUS imaging studies have also confirmed the same pattern of distribution of these lipid-rich and large PB plaques.^{9,10} For example, in the PROSPECT ABSORB study,¹¹ which included patients with large PB detected by IVUS, most treated lesions were located in the two most proximal segments in the coronary vessel, and approximately one-third were located in each of the three major coronary vessels. In the LRP study, by protocol, all obstructive lesions were treated at the index procedure; 47% of the PCIs at baseline were in the LAD, 26% in the LCX, and 25% in the RCA. Even though most of the index PCIs took place in the LAD, revascularizations during follow-up were also performed most frequently in the LAD.

There have been some natural history studies using non-invasive imaging such as computed tomography angiography (CTA) exploring whether the vessel location is associated with major coronary events.

In a CTA study involving 1127 patients, Min *et al.*¹² found that the proximal LAD and number of diseased vessels were predictors of all-cause mortality at 1 year. Similarly, Pundziute *et al.*¹³ reported that patients with coronary lesions in the LAD had a greater risk of coronary events (i.e., cardiac death, non-fatal MI, unstable angina requiring hospitalization, and revascularization) in both univariate and multivariate analyses. In line with LRP study observations, the plaque characteristics observed in CTA studies that conferred high risk to future cardiac events included the presence of low-attenuation plaques (i.e., lipid-rich plaque) and the degree of obstruction. Nakanishi *et al.*¹⁴ reported that the number of low-attenuation plaques in the LAD was an independent predictor of ACS.

Limitations

Despite being the largest-ever natural history study using IVUS imaging, the number of plaque-level events in the LRP study was relatively small. Second, this study was carried out as a *post hoc* analysis from



the parent study and was not powered for vessel-level comparison of the relationship between the maxLCBI_{4mm} and non-culprit events. Further studies will be required to evaluate the correlation of NIRS-IVUS maxLCBI_{4mm} >400 with other plaque-event predictors on an epicardial vessel level.

2 years. Non-culprit segments in the LAD with maxLCBI_{4mm} values >400 were more frequently associated with plaque-level events than the lipid-rich segments in the other epicardial vessels. Because most events occurred in the LAD, screening of this vessel with NIRS-IVUS may help identify patients requiring intensive medical treatment and closer follow-up.

Conclusions

In the LRP study, plaque-level events were commonly found in the LAD location, especially in untreated lipid-rich plaques within the first

Supplementary data

Supplementary data are available at *European Heart Journal - Cardiovascular Imaging* online.

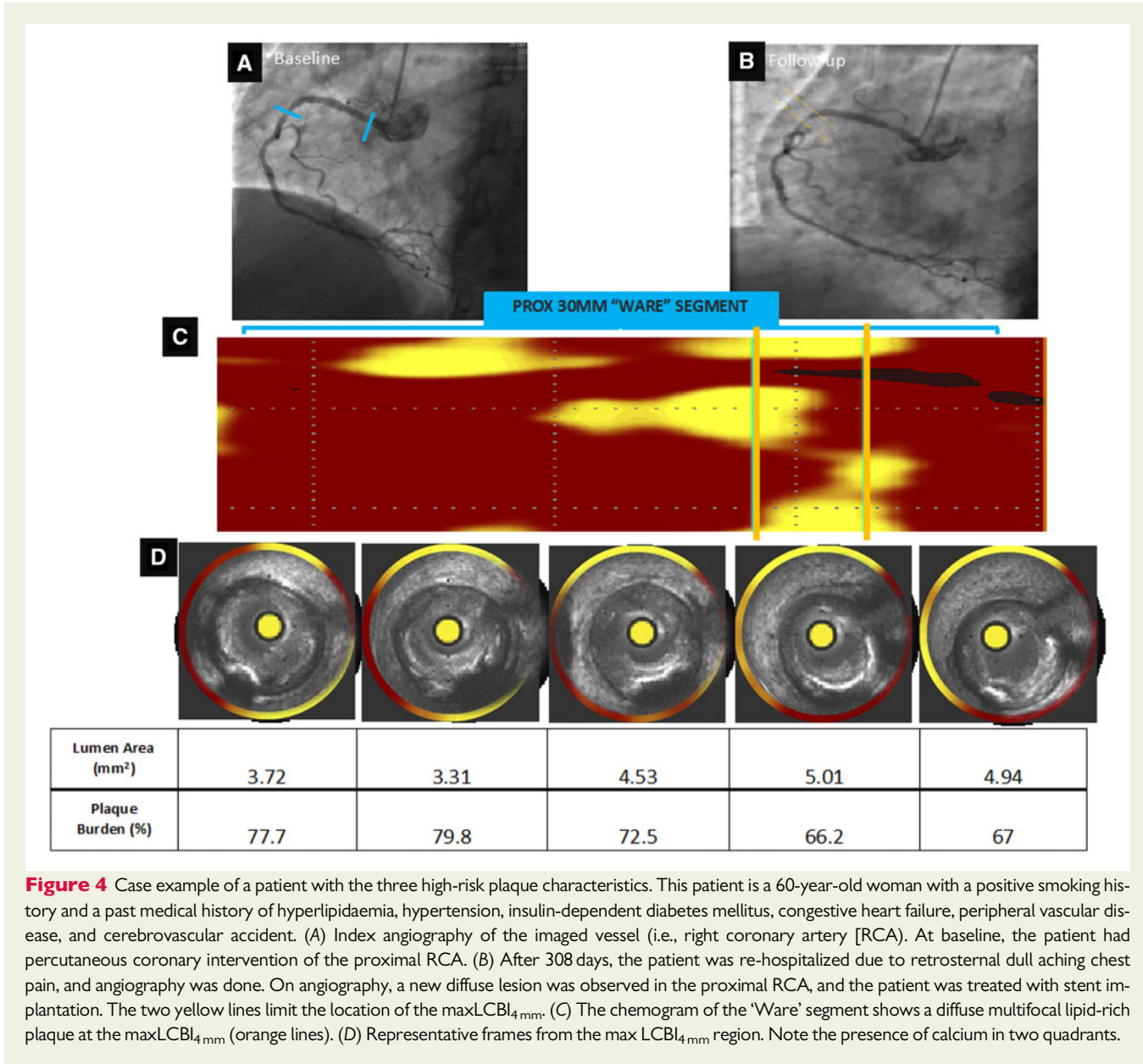


Figure 4 Case example of a patient with the three high-risk plaque characteristics. This patient is a 60-year-old woman with a positive smoking history and a past medical history of hyperlipidaemia, hypertension, insulin-dependent diabetes mellitus, congestive heart failure, peripheral vascular disease, and cerebrovascular accident. (A) Index angiography of the imaged vessel (i.e., right coronary artery [RCA]). At baseline, the patient had percutaneous coronary intervention of the proximal RCA. (B) After 308 days, the patient was re-hospitalized due to retrosternal dull aching chest pain, and angiography was done. On angiography, a new diffuse lesion was observed in the proximal RCA, and the patient was treated with stent implantation. The two yellow lines limit the location of the maxLCBI_{4mm}. (C) The chemogram of the 'Ware' segment shows a diffuse multifocal lipid-rich plaque at the maxLCBI_{4mm} (orange lines). (D) Representative frames from the max LCBI_{4mm} region. Note the presence of calcium in two quadrants.

Conflict of interest: R.W., C.D.M., H.M.G.-G., and R.T. were Principal Investigator, European Principal Investigator, Responsible Officer Core Laboratory NIRS-IVUS and angiographic analysis, Worldwide Study Coordinator of the Lipid Rich Trial, sponsored by Infraredx-Nipro, Bedford, MA, USA. H.M.G.-G. reports the following institutional grant support: Biotronik, Boston Scientific, Medtronic, Abbott, Neovasc, Shockwave, Phillips, and Corflow. C.D.M. is the recipient of research grants (through the Department of Clinical and Experimental Medicine of the University of Florence) from AMGEN, Behring, Chiesi, Daiichi Sankyo, Edwards, Medtronic, and Shockwave. Z.A.A. reports grants from NIH/NHLBI, Abbott Vascular, and Cardiovascular Systems Inc.; personal fees from Amgen, Astra Zeneca, and Boston Scientific; and equity from Shockwave Medical. G.S.M. reports honoraria from Boston Scientific and Philips. R.W. reports serving on the advisory boards of Abbott Vascular, Amgen, Boston Scientific, Cardioset, Cardiovascular Systems Inc., Medtronic, Philips, and Pi-Cardia Ltd.; being a consultant for Abbott

Vascular, Amgen, Biotronik, Boston Scientific, Cardioset, Cardiovascular Systems Inc., Medtronic, Philips, Pi-Cardia Ltd., and Transmural Systems; receiving grant support from AstraZeneca, Biotronik, Boston Scientific, and Chiesi; serving on the speakers bureaus of AstraZeneca and Chiesi, and being an investor in MedAlliance and Transmural Systems. All other authors declared no conflict of interest.

Funding

This substudy received no funding. The LRP trial was sponsored by Infraredx, Bedford, MA, USA.

References

1. Campos CM, Costa F, Garcia-Garcia HM, Bourantas C, Suwannasom P, Valgimigli M et al. Anatomic characteristics and clinical implications of angiographic coronary thrombus: insights from a patient-level pooled analysis of SYNTAX, RESOLUTE, and LEADERS Trials. *Circ Cardiovasc Interv* 2015;8:e002279.

2. García-García HM, Goedhart D, Schuurbiers JCH, Kukreja N, Tanimoto S, Daemen J et al. Virtual histology and remodelling index allow in vivo identification of allegedly high-risk coronary plaques in patients with acute coronary syndromes: a three vessel intravascular ultrasound radiofrequency data analysis. *EuroIntervention* 2006;2:338–44.
3. Bax AM, van Rosendael AR, Ma X, van den Hoogen IJ, Gianni U, Tantawy SW et al; PARADIGM Investigators. Comparative differences in the atherosclerotic disease burden between the epicardial coronary arteries: quantitative plaque analysis on coronary computed tomography angiography. *Eur Heart J Cardiovasc Imaging* 2021;22:322–30.
4. Feldmann KJ, Goldstein JA, Marinescu V, Dixon SR, Raff GL. Disparate impact of ischemic injury on regional wall dysfunction in acute anterior vs inferior myocardial infarction. *Cardiovasc Revasc Med* 2019;20:965–72.
5. Ibanez B, James S, Agewall S, Antunes MJ, Buccarelli-Ducci C, Bueno H et al. 2017 ESC Guidelines for the management of acute myocardial infarction in patients presenting with ST-segment elevation: the Task Force for the management of acute myocardial infarction in patients presenting with ST-segment elevation of the European Society of Cardiology (ESC). *Eur Heart J* 2018;39:119–77.
6. Waksman R, Di Mario C, Torguson R, Ali ZA, Singh V, Skinner WH et al. Identification of patients and plaques vulnerable to future coronary events with near-infrared spectroscopy intravascular ultrasound imaging: a prospective, cohort study. *Lancet* 2019;394:1629–37.
7. Waksman R, Torguson R, Spad M-A, Garcia-Garcia H, Ware J, Wang R et al. The Lipid-Rich Plaque study of vulnerable plaques and vulnerable patients: study design and rationale. *Am Heart J* 2017;192:98–104.
8. Bourantas CV, Zanchin T, Torii R, Serruys PW, Karagiannis A, Ramasamy A et al. Shear stress estimated by quantitative coronary angiography predicts plaques prone to progress and cause events. *JACC Cardiovasc Imaging* 2020;13:2206–19.
9. Wykrzykowska JJ, Mintz GS, Garcia-Garcia HM, Maehara A, Fahy M, Xu K et al. Longitudinal distribution of plaque burden and necrotic core-rich plaques in non-culprit lesions of patients presenting with acute coronary syndromes. *JACC Cardiovasc Imaging* 2012;5:S10–8.
10. Hong M-K, Mintz GS, Lee CW, Lee B-K, Yang T-H, Kim Y-H et al. The site of plaque rupture in native coronary arteries: a three-vessel intravascular ultrasound analysis. *J Am Coll Cardiol* 2005;46:261–5.
11. Stone GW, Maehara A, Ali ZA, Held C, Matsumura M, Kjøller-Hansen L et al. Percutaneous coronary intervention for vulnerable coronary atherosclerotic plaque. *J Am Coll Cardiol* 2020;76:2289–301.
12. Min JK, Shaw LJ, Devereux RB, Okin PM, Weinsaft JW, Russo DJ et al. Prognostic value of multidetector coronary computed tomographic angiography for prediction of all-cause mortality. *J Am Coll Cardiol* 2007;50:1161–70.
13. Pundziute G, Schuijf JD, Jukema JW, Boersma E, de Roos A, van der Wall EE et al. Prognostic value of multislice computed tomography coronary angiography in patients with known or suspected coronary artery disease. *J Am Coll Cardiol* 2007;49:62–70.
14. Nakanishi K, Fukuda S, Shimada K, Ehara S, Inanami H, Matsumoto K et al. Non-obstructive low attenuation coronary plaque predicts three-year acute coronary syndrome events in patients with hypertension: multidetector computed tomographic study. *J Cardiol* 2012;59:167–75.